

Scratch resistance anisotropy in biaxially oriented polypropylene and poly(ethylene terephthalate) films

H.-Y. Nie^{*}, M.J. Walzak, N.S. McIntyre

Surface Science Western, Room G-1, Western Science Centre, The University of Western Ontario, London, Ont., Canada N6A 5B7

Received 17 April 2006; accepted 20 April 2006

Available online 24 May 2006

Abstract

Using a diamond-tipped stylus, scratch tests were conducted on biaxially oriented polypropylene and poly(ethylene terephthalate) films in the two draw directions, i.e., the machine-direction (MD) and the transverse-direction (TD) along which the draw ratios are different. Atomic force microscopy study of those scratches revealed a significant anisotropy in the scratch resistance between the MD and TD for both of the polymer films. We confirmed that the scratch resistance of polymer strands is closely related to the draw ratios, which determine the mechanical strength and optical clarity of biaxially oriented polymer films.

© 2006 Elsevier B.V. All rights reserved.

PACS: 62.20.Fe; 68.37.Tj; 68.47.Mn

Keywords: Biaxially oriented polymer film; BOPP; PET; Draw ratio; Scratch resistance anisotropy

1. Introduction

Since the introduction of atomic force microscopy (AFM) [1], a mechanical probe technique that provides three-dimensional information on surface morphology, it has been used extensively in the characterization of polymer surfaces. AFM has made it possible to investigate both surface morphology at the molecular level [2] and nanoscale mechanical properties [3]. We have used AFM to study the inherent morphology and the effect of surface modification on a biaxially oriented polypropylene (BOPP) film [4,5]. Surface treatment of BOPP in a UV/ozone environment results in oxidation of the polymer surface, improving the surface wettability for adhesion and printing applications [4,6]. In the course of these studies, we also observed scratches on the BOPP film and proved that they were caused by shear deformation during the rolling process, most likely from protruding particles on rollers [5].

Bidirectional drawing of polymer resin is a standard industrial method of fabricating polymer films for various applications including flexible packaging [7]. In the fabricating

process, the polymer is first drawn in the machine-direction (MD) and sequentially in the transverse-direction (TD). Biaxially oriented polymer films are usually regarded as semi-crystalline because of the ordering of the polymer strands in the film due to the drawing process. Lupke et al. has thoroughly studied the development of polymer strand orientation in sequentially oriented BOPP films with different draw ratios [8]. For oriented polymer films, the Young's modulus increases with draw ratio [9] and the molecular orientation [10] determines their physical properties. Biaxially oriented polymer films are characterized by their high mechanical strength and optical clarity, usually due to the high draw ratios. Different approaches of characterizing the orientation of biaxially oriented polymer films are important to understand the relationship between the structure and the properties [8–13].

Scratch resistance is a measure of a material's response to shear deformation imposed by another, harder, material [14–16]. In this paper, we report that simple scratch tests, using a diamond tip and a controlled applied force, revealed scratch resistance anisotropy in a BOPP film and another biaxially oriented polymer film, poly(ethylene terephthalate) (PET). The observed anisotropy for the two films suggests a significant difference in the response of the biaxially oriented polymer films to shear deformation parallel to the MD and

^{*} Corresponding author. Tel.: +1 519 661 2173; fax: +1 519 661 3709.

E-mail address: hnie@uwo.ca (H.-Y. Nie).

TD. We confirmed that higher draw ratios make a stronger polymer film as the polymer strands aligned in the draw direction have a higher scratch resistance to shear deformation applied perpendicularly. Although biaxially oriented polymer films have been studied by several methods [8] such as infrared spectroscopy [11,13], differential scanning calorimetry [12] and small-angle wide-angle X-ray scattering [9,10], to our best knowledge, there has been no report on scratch resistance anisotropy for a biaxially oriented polymer film. Therefore, our results confirm the connection between mechanical properties and draw ratios for biaxially oriented polymer films.

2. Materials and methods

Thermally extruded, biaxially oriented isotactic polypropylene (PP) film (0.03 mm thick) was used in this study. The PP film was produced from a homopolymer resin (molecular weight $M_w = 1.9 \times 10^5$, polydispersity = 6.0). The base resin contains 500–1000 ppm each of an inorganic acid scavenger and a high-molecular weight phenolic antioxidant. The PP was produced on a tenter frame film line and quenched at 45 °C prior to orientation. The BOPP film was formed with MD and TD draw ratios of 5.2:1 and 9:1, respectively.

The 0.1 mm thick PET film was fabricated from a homopolymer resin with a degree of polymerization of 100 ($M_w = 2.5 \times 10^5$). The PET base resin contained ~300 ppm of residual metal catalyst and 50 ppm of an organometallic thermal stabilizer. Biaxially oriented film was produced from this resin on a tenter-frame film line. The MD draw ratio was 3.4:1 and the TD draw ratio 4.6:1. Both of the polymer films described above were received from 3M Company at St. Paul, MN, USA.

Scratch tests were performed using a diamond-tipped, stylus-type, surface profiler (P-10, Tencor) capable of providing applied forces in the range 0.01–0.49 mN. The nominal radius of diamond tip was 2 μm . Scratches were created parallel to the MD and TD by moving the sample against the tip under various applied forces at a fixed scan speed of 50 $\mu\text{m}/\text{s}$ for all experiments. The scratches were created under a relative humidity of ~40%.

A Topometrix Explorer model AFM was employed in this study to analyze the scratches created on the polymer films. For dynamic force mode AFM measurements, a silicon cantilever with a spring constant of ~40 N/m was used. The cantilever was 125 μm long, 30 μm wide and 3.7 μm thick. The tip apex radius was nominally 10 nm. Dynamic force mode AFM works by maintaining a certain damped oscillation amplitude (usually 50% of the amplitude in free space) of the cantilever while the tip scans the surface. The AFM feedback system adjusts the distance between the tip and sample so that the damped oscillation amplitude remains constant. This adjustment of the separation between the tip and surface allows the AFM to image surface morphology. All images were obtained in air with a relative humidity around ~40%.

3. Results and discussion

Shown in Fig. 1(a) and (b) are typical AFM images of the BOPP film and PET film, respectively. The MD is indicated in the image; and the TD is perpendicular to the MD. It is evident in Fig. 1(a) that the BOPP film is characterized by nanometer-scale fiber-like network structures [17,18], which are formed during the biaxial drawing process [8]. In the drawing process, polymer strands align in the drawing direction, i.e., first in the MD and then in the TD. Therefore, polymer strands aligned in the MD direction are subjected to re-alignment when they are drawn subsequently in the TD. This way, the resultant surface morphology of the polymer film is characterized by a network-like structure. This development of the fiber-like network structure seen on the BOPP film has been detailed by Lupke et al. [8].

In contrast, as seen in Fig. 1(b), there are no apparent surface features reflecting the drawing process for the PET film, which is, instead, characterized by particle-like features. These features, having an apparent size of ~10 nm, are believed to represent small crystallites of PET formed in the biaxially drawing process [19]. It is clear that the surface morphology is drastically different between the two polymer films, although both were fabricated using a biaxial drawing process. This

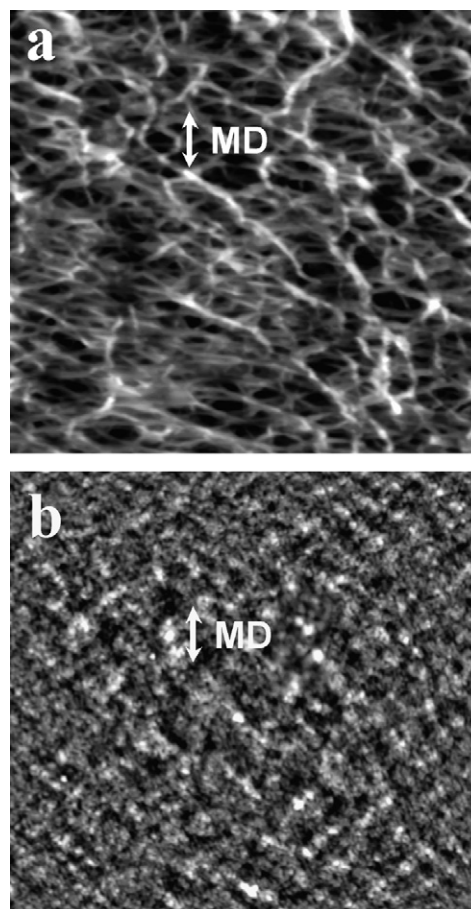


Fig. 1. AFM images (scan area, 2 $\mu\text{m} \times 2 \mu\text{m}$) showing typical surface morphology for BOPP (a) and PET (b). The MD is indicated in the image. The gray scale for (a) and (b) is 20 and 6 nm, respectively.

difference in surface morphology should reflect the differences between the two polymers at the molecular level. Also, the surface mechanical properties are different between the two polymer films: PET is very prone to shear deformation as the surface was modified by an AFM tip under typical contact-mode AFM operation conditions as reported by Dinelli et al. [19]; in contrast, we did not encounter this same deformation on BOPP films.

Shown in Fig. 2 are two line profiles extracted from the respective AFM images shown in Fig. 1, one from each of the BOPP (dotted line) and the PET (solid line). The arithmetic roughnesses calculated from the line profiles of the BOPP and PET are 3.16 and 0.97 nm, respectively. The root mean square (RMS) roughness is 4.02 nm for the BOPP and 1.13 nm for the PET. The area averaged arithmetic roughnesses estimated from the entire AFM images shown in Fig. 1(a) and (b) are 3.19 and 0.97 nm for the BOPP and PET films, respectively. The area averaged RMS roughness for the BOPP film is 4.05 and 1.24 nm for the PET films. AFM analysis of the surfaces of the two polymer films revealed that the PET surface is much smoother than the BOPP surface because of the lack of fiber-like structures on the PET surface.

In order to probe the differences in scratch resistance for these biaxially oriented polymer films using, scratches were created in both the MD and TD a diamond tip under controlled normal forces. AFM images of the scratches created on the BOPP and PET films are shown in Figs. 3 and 4, respectively, with the images of the scratches made parallel to the MD shown in the left column and those made parallel to the TD in the right column. The applied force used in ranges from 0.06 mN (top row) to 0.49 mN (bottom row). The draw direction (i.e., MD or TD) is indicated in the AFM images in the top row and the applied force is indicated in the AFM images in the left column. The same gray scale is used for each pair of images of scratches made using the same applied force. This convention allows direct comparison of the scratches created in the MD and TD using the same applied force. The scratches were created by moving the polymer film against the diamond-tipped stylus of the profiler. By placing the MD or TD of the polymer film parallel to the direction of movement of the sample stage, we were able to create scratches in the film parallel to each draw direction. In the images shown in Figs. 3 and 4, the scratch is made from bottom to top.

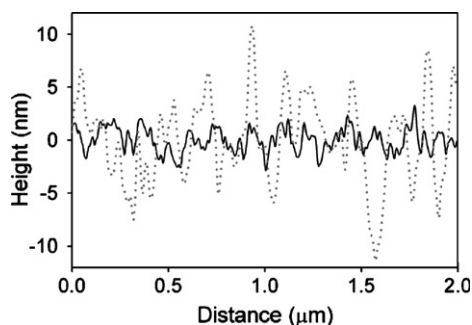


Fig. 2. Profiles for BOPP (dotted line) and PET (solid line) isolated from Fig. 1(a) and (b), respectively.

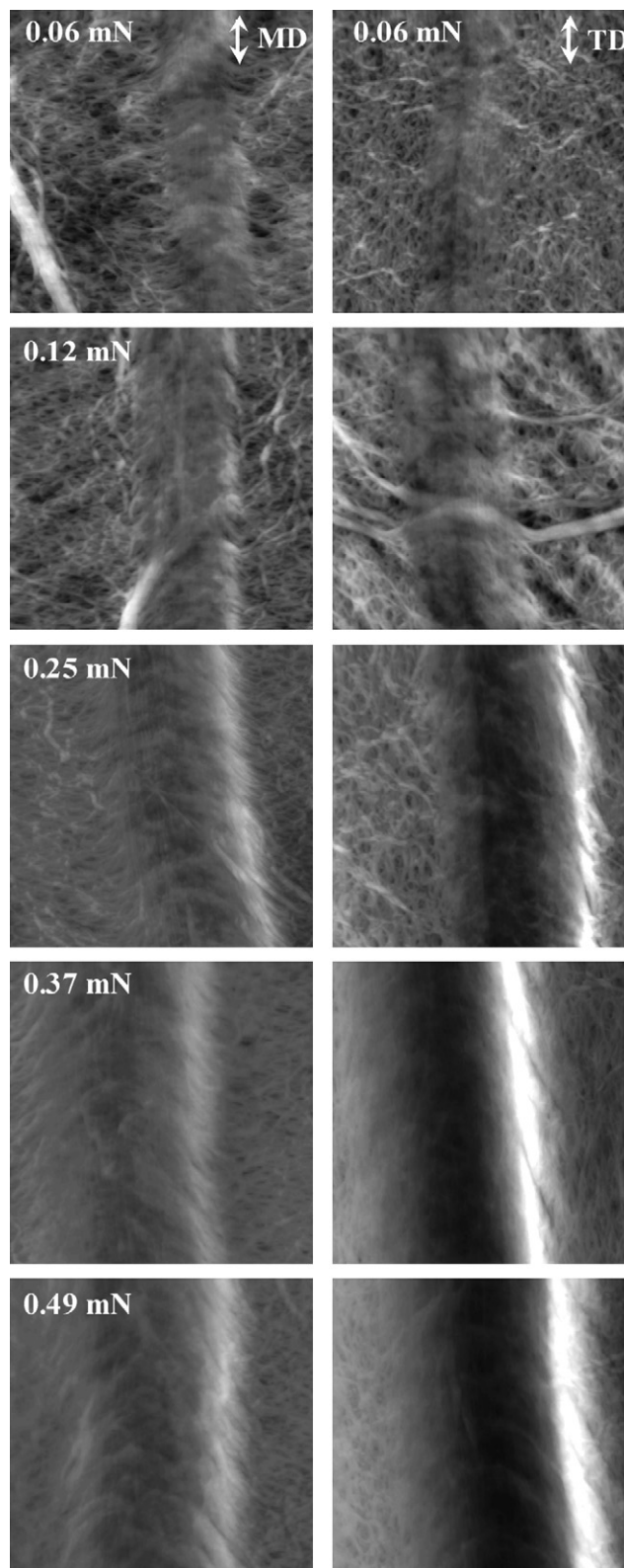


Fig. 3. AFM images (scan area, $2.5 \mu\text{m} \times 2.5 \mu\text{m}$) for scratches created on a BOPP film parallel to the MD (left column) and TD (right column) under different applied forces. The two images at each row are for the scratches created under the same applied force parallel to the MD and TD, which is 0.06, 0.12, 0.25, 0.37, and 0.49 mN, respectively, from the top row to the bottom row. The gray scale for each pair of images is kept the same so that the difference in depth is presented more clearly. The gray scale for the rows from the top to the bottom is 78, 75, 126, 180, and 215 nm, respectively.

As shown in Fig. 3, at applied forces of 0.06 and 0.12 mN, only the fiber-like BOPP surface was modified and there were no significant differences between the scratches created in the MD and TD. At these low applied forces, there appears to be no well-defined depth to the scratch because the roughness of the BOPP surface is large compared to the deformation caused by the scratching. Under applied forces between 0.25 and 0.49 mN, clear differences in depth between the scratches created along the MD and TD emerge for the BOPP film. The scratches created parallel to the MD (draw ratio: 5.2:1) are shallower than those created parallel to the TD (draw ratio: 9:1). Note that the polymer strands tend to align with the draw direction; therefore, to make a scratch parallel to the MD, we believe that the diamond tip mainly needs to deform or displace polymer strands aligned in the perpendicular direction, i.e., TD, and vice versa. Therefore, the results shown in Fig. 3 suggest that it is harder to generate scratches perpendicular to the direction having a higher draw ratio. This is consistent with the increase in the Young's modulus with increasing draw ratio [9].

For the PET film, the difference in the depths of the scratches created between the TD and the MD emerges at an applied force of only 0.12 mN, as shown in Fig. 4. The scratch created parallel to the MD is much shallower than that created parallel to the TD, indicating that the polymer strands aligned in the TD (draw ratio: 4.6:1) have a much higher scratch resistance than do those aligned in the MD (draw ratio 3.5:1). It is thus clear that even though there are no apparent directional characteristics from the surface morphology of the PET film (Fig. 1(b)), the film has the characteristic scratch resistance anisotropy that originates from the difference in the draw ratios between the TD and MD. Therefore, for a biaxially oriented polymer film that shows no directional difference in the surface morphology, scratch tests can be used to identify the orientation or to determine if the MD and TD draw ratios are different. Therefore, the scratch test appears useful for characterizing mechanical property anisotropy in polymer films.

Other characteristics of the PET film were also noted on scratching. As can be seen in Fig. 4, regular bundles are formed in the scratches created on the PET film, seen as wave-like formations. A modified AFM image of the scratch created on the PET film in the MD under an applied force of 0.37 mN is presented in Fig. 5(a): in order to more clearly visualize the bundle features, which are masked by the large dynamic height range in the original image, we removed the height information in the horizontal direction. Clearly shown in the modified image in Fig. 5(a), the bundles are seen arcing in the scratch direction. The corrugation height of the bundles is several nanometers. Bundle formation is a common phenomenon for crystalline polymer films subjected to shear deformation [20,21]. When subjected to shear deformation as applied from the scratching tip, the polymer chains are compressed and rearranged to produce an opposing force which tries to restore the original state. After a certain amount of material has built up due to the compression of polymer chains, the opposing restoring force reaches the same value as the shearing force applied through the tip and the tip skips over the polymer buildup. The bundles are

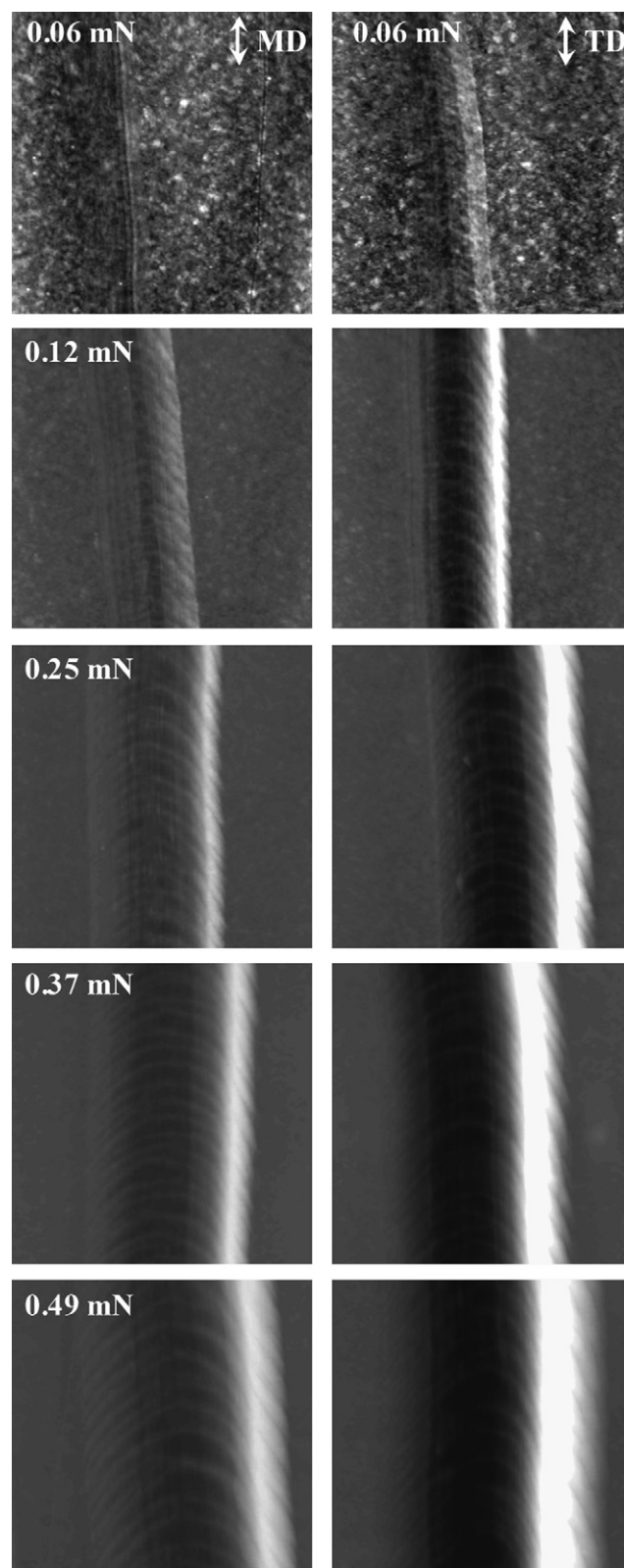


Fig. 4. AFM images (scan area, $2.5 \mu\text{m} \times 2.5 \mu\text{m}$) for scratches created on a PET film parallel to the MD (left column) and TD (right column) under different applied forces. The two images at each row are for the scratches created under the same applied force parallel to the MD and TD, which is 0.06, 0.12, 0.25, 0.37, and 0.49 mN, respectively, from the top row to the bottom row. The gray scale for each pair of images is kept the same so that the difference in depth is presented more clearly. The gray scale for the rows from the top to the bottom is 12, 58, 138, 231, and 290 nm, respectively.

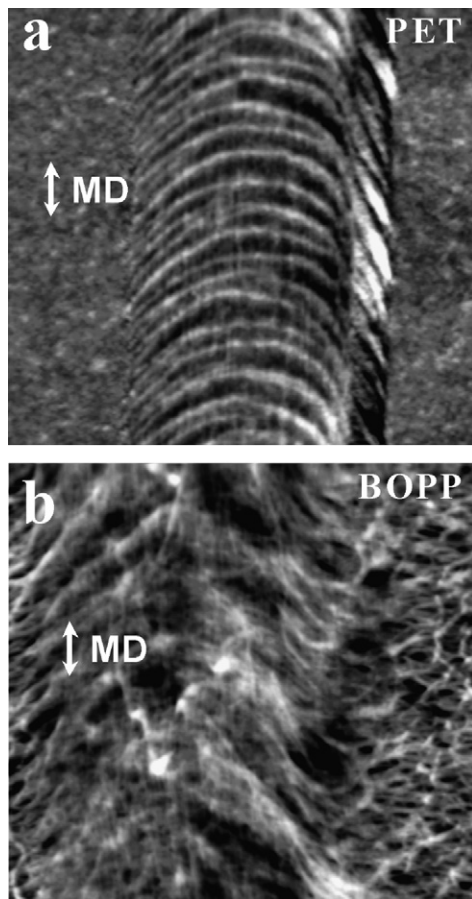
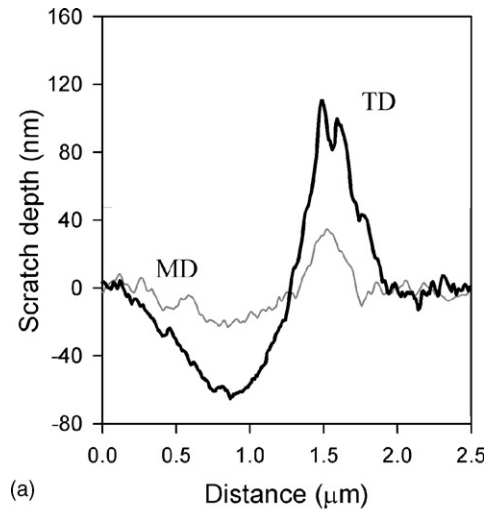


Fig. 5. AFM images (scan area, $2.5 \mu\text{m} \times 2.5 \mu\text{m}$) treated by removing the height information across the horizontal direction to emphasize the bundle formation on the scratch created in the MD for PET (a) and BOPP (b). The original image for (a) and (b) is Fig. 4 (0.37 mN, MD) and Fig. 3 (0.37 mN, MD), respectively. The gray scale is 15 and 25 nm for (a) and (b), respectively.

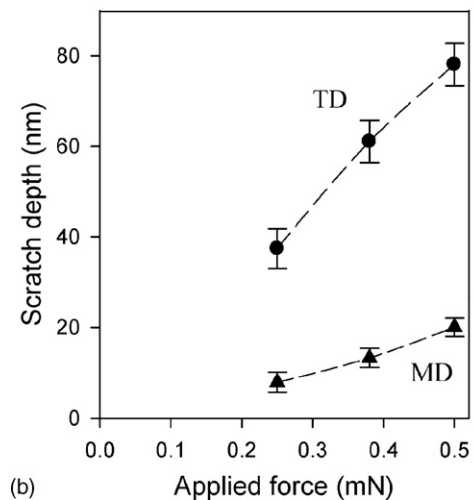
left behind, the result of plastic deformation of the polymer surface [20,21].

The bundle formation is not seen as clearly on the BOPP. A modified AFM image of the scratch created in the MD on the BOPP film (Fig. 3, 0.37 mN) is shown in Fig. 5(b). The height distribution across the scratch has been removed so that the scratched surface can be visualized more clearly. Vague and irregular bundles can be seen in Fig. 5(b), which are hindered by the relatively rough BOPP surface. As reported previously, thinner fibers parallel to the scratch direction are visible on the scratch [5]. The difference in bundle formation between the two polymer surfaces suggests that the particle-like structure of the PET film is more easily rearranged than the fiber-like network structure of the BOPP film.

Typical line profiles of the scratch created with an applied pressure of 0.37 mN parallel to the MD and TD for the BOPP and PET are shown in Figs. 6(a) and 7(a), respectively. As seen in the profiles and the images (0.37 mN) in Figs. 3 and 4, there is a buildup of polymer material on only one side of the scratch. These buildups are found on the same side of all scratches we created, which leads us to believe that the buildup is caused by an irregularity in the diamond tip we



(a)



(b)

Fig. 6. Typical profiles for scratches created on a BOPP film in the MD and TD under the applied force of 0.37 mN (a) and the estimated depths from the AFM images shown in Fig. 3 for the scratches created under applied forces of 0.25, 0.37 and 0.49 mN (b). The broken lines are used to guide the eye.

used to create the scratches. The buildups are more pronounced for scratches created on the PET film. It is evident that the two polymer films were plastically deformed and that the buildup is most likely an accumulation of compressed polymer materials. From the profiles shown in Figs. 6(a) and 7(a), one can see that the scratch is deeper and the buildup higher for the scratches created in the TD than in the MD for both BOPP and PET. It appears that, under the same conditions, the biaxially oriented polymers are scratched more deeply when the tip traverses in the TD than in the MD. As the main resistance comes from polymer strands that are aligned perpendicular to the direction of motion of the diamond tip, it is clear that the scratch resistance of polymer strands aligning in the TD is much larger than that in the MD.

An increase in the depth of the scratch with increased applied force is shown in Figs. 6(b) and 7(b) for the BOPP and PET films, respectively. The scratch depths and their standard deviations were estimated using fifteen typical

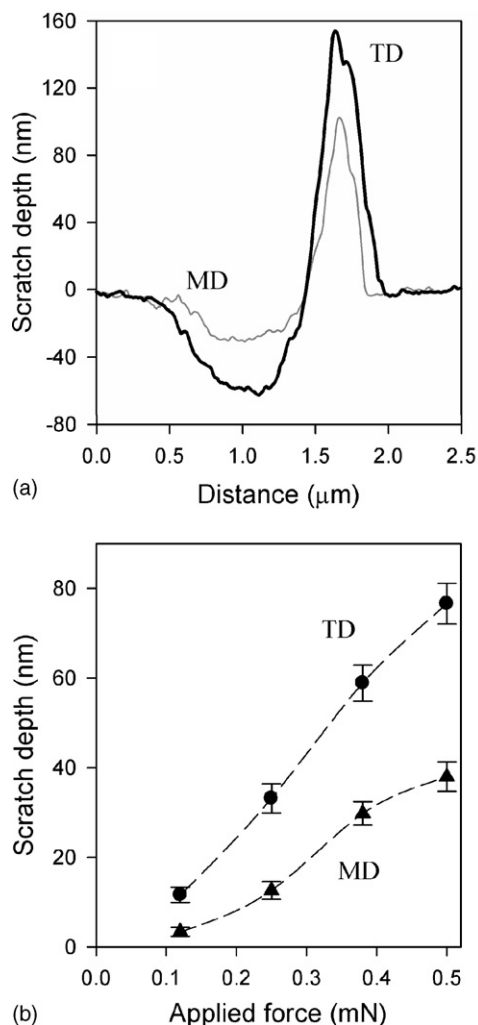


Fig. 7. Typical profiles for scratches created on a PET film in the MD and TD under the applied force of 0.37 mN (a) and the estimated depths from the AFM images shown in Fig. 4 for the scratches created under applied force of 0.12, 0.25, 0.37 and 0.49 mN (b). The broken lines are used to guide the eye.

profiles from the corresponding AFM images shown in Figs. 3 and 4. The depths of the scratches created on the BOPP film in the MD and TD are significantly different, as shown in Fig. 6(b). For example, for the scratches created using an applied force of 0.49 mN, the depths of the scratches created in the MD and TD are 20 ± 2 and 78 ± 5 nm, respectively. The similar trend is also observed on the PET film as shown in Fig. 7(b). For example, the scratches created on the PET film using an applied force of 0.49 mN (Fig. 7 (b)) are 38 ± 3 and 77 ± 5 nm deep in the MD and TD, respectively. However, we observed a larger increase in the depth of the scratches with increased applied force for scratches created in the TD for both BOPP and PET (Figs. 6(b) and 7(b)). It is clear, therefore, that this simple scratch test provides useful information regarding the response of polymer strands to shear deformation depending on their alignment in either the MD or the TD. The response to the deformation is dependent on the draw ratio in the alignment direction. It is worth noting that although the

surface morphology of the PET as measured by AFM shows no difference between the MD and TD directions, significant differences are seen in the scratch resistances between the two draw directions.

Although the polymer film was plastically deformed during the formation of the scratches, one still may apply the Hertzian model [22,23] to extract useful information regarding the deformation during the shear deformation. For the system of a sphere (diamond-tipped stylus) with a radius R indenting a much softer plane (polymer film) having a Young's modulus E and a Poisson's ratio σ , the deformation depth d under an applied force F is $d = (FD)^{2/3}(R)^{-1/3}$, where $D = 3(1 - \sigma^2)/(4E)$. Assuming that the Young's modulus and Poisson's ratio for the BOPP film are 2 GPa and 0.3 [24], respectively and using the known radius of 2 μm for the diamond tip, the Hertzian model predicts deformation depths of 152, 201 and 694 nm using an applied force of 0.25, 0.37 and 0.49 mN, respectively. The observed depths of the scratches created using these applied forces on the BOPP film were much smaller than the calculated values using the Hertzian model. This is generally true because the scratching involves both elastic and plastic deformations and the generation of a scratch is solely the result of the plastic deformation [25]. The elastic restoration and the re-flow of the deformed polymer after the load is removed could explain the much shallower observed scratch depth [26]. The depth of the scratches is determined by the intrinsic properties (such as Young's modulus and viscosity) of the polymer film that respond to the shear deformation.

Based on the results of scratch tests conducted parallel to the MD and TD for these two biaxially oriented polymer films, it is clear that their mechanical response to shear deformation is anisotropic between the MD and TD. We relate this anisotropy to the structural difference in the biaxially oriented polymer film, which is most likely a result of the different draw ratios between the MD and the TD. For the BOPP film the draw ratio in the TD (9:1) is 73% larger than that in the MD (5.2:1). The PET film has a draw ratio in the TD (4.6:1) 35% larger than that in the MD (3.4:1). Therefore, both polymer films were stretched more in the TD than in the MD. According to Lupke et al. [8], a higher TD draw ratio results in an alignment of polymer strands in the drawing direction. As the polymer strands tend to align in the draw direction, scratching the film in the direction parallel to that with the higher draw ratio is easier and results in a deeper scratch than scratching perpendicular to the alignment. This is consistent with the fact that the Young's modulus of the polymer strands increases with increasing draw ratio [9]. We confirmed this hypothesis using another BOPP film having similar MD and TD draw ratios [27], where we observed scratch depth of ~ 20 nm under an applied force of 0.49 mN for scratches created in both MD and TD. In addition, Dasari et al. conducted scratch tests on polypropylene bars made by injection molding and no apparent scratch resistance anisotropy was reported [28,29]. It is thus clear that scratch resistance anisotropy is characteristic for biaxially oriented polymer films having different MD and TD draw ratios.

4. Conclusions

Anisotropy in the scratch resistance between the machine-direction (MD) and transverse-direction (TD) was observed for biaxially oriented PP and PET films where the TD draw ratios were 73% and 35% larger than their respective MD draw ratios. The deeper scratches created in the TD using a diamond tip as compared to those created in the MD suggest that, for a biaxially oriented polymer film, a higher draw ratio in the TD results in a stronger mechanical resistance to shear deformation perpendicular to that direction. This leads us to conclude that scratch resistance mainly arises from the resistance of polymer strands oriented perpendicular to the scratch direction: the diamond tip has to break or move those perpendicular polymer strands to make a scratch on the film.

References

- [1] G. Binnig, C.F. Quate, Ch. Gerber, *Phys. Rev. Lett.* 56 (1986) 930.
- [2] A. Stamouli, S. Kafi, D.C.G. Klein, T.H. Oosterkamp, J.W.M. Frenken, R.J. Cogdell, T.J. Aartsma, *Biophys. J.* 84 (2003) 2483.
- [3] Y.F. Dufrene, W.R. Barger, J.-B.D. Green, G.U. Lee, *Langmuir* 13 (1997) 4779.
- [4] H.-Y. Nie, M.J. Walzak, B. Berno, N.S. McIntyre, *Appl. Surf. Sci.* 144/145 (1999) 627.
- [5] H.-Y. Nie, M.J. Walzak, B. Berno, N.S. McIntyre, *Langmuir* 15 (1999) 6484.
- [6] M.J. Walzak, S. Flynn, R. Foerch, J.M. Hill, E. Karbasheski, A. Lin, M. Strobel, *J. Adhes. Sci. Technol.* 9 (1995) 1229.
- [7] W.J. Kissel, J.H. Han, J.A. Meyer, in: H.G. Karian (Ed.), *Handbook of Polypropylene and Polypropylene Composites*, Marcel Dekker, New York, 2003, p. 11.
- [8] T. Lupke, S. Dunger, J. Sanze, H.-J. Radusch, *Polymer* 45 (2004) 6861.
- [9] A. Peterlin, *J. Appl. Phys.* 48 (1977) 4099.
- [10] J.M. Strobel, S. Nam, *J. Appl. Polym. Sci.* 42 (1991) 159.
- [11] K.C. Cole, H.B. Daly, B. Sanschagrin, K.T. Nguyen, A. Ajji, *Polymer* 40 (1999) 3505.
- [12] M.B. Elias, R. Machado, S.V. Canevarolo, *J. Therm. Anal. Cal.* 59 (2000) 143.
- [13] N. Overall, D. MacKerron, D. Winter, *Polymer* 43 (2002) 4217.
- [14] V. Jardret, P. Morel, *Prog. Org. Coat.* 48 (2003) 322.
- [15] B.J. Briscoe, S.K. Sinha, *Mat-wiss. u. Werkstofftech.* 34 (2003) 989.
- [16] W.D. Shen, J. Sun, Z.Q. Liu, W.J. Mao, J.D. Nordstrom, P.D. Ziemer, F.N. Jones, *JCT Res.* 1 (2004) 117.
- [17] M. Strobel, V. Jones, C.S. Lyons, M. Ulsh, M.J. Kushner, R. Dorai, M.C. Branch, *Plasma Polym.* 8 (2003) 61.
- [18] S. Guimond, M.R. Wertheimer, *J. Appl. Polym. Sci.* 94 (2004) 1291.
- [19] F. Dinelli, H.E. Assender, K. Kirov, O.V. Kolosov, *Polymer* 41 (2000) 4285.
- [20] O.M. Leung, M.C. Goh, *Science* 255 (1992) 64.
- [21] Z. Elkaakour, J.P. Aime, T. Bouhacina, C. Odin, T. Masuda, *Phys. Rev. Lett.* 73 (1994) 3231.
- [22] L.D. Landau, E.M. Lifshitz, *Theory of Elasticity*, Pergamon Press, London, 1959, pp. 30.
- [23] K.L. Johnson, *Contact Mechanics*, Cambridge University Press, Cambridge, 1985, pp. 90.
- [24] W. Brostow, J. Kubat, M.M. Kubat, in: J.E. Mark (Ed.), *Physical Properties of Polymers Handbook*, American Institute of Physics, New York, 1996, p. 331.
- [25] B.Y. Du, M.R. VanLandingham, Q.L. Zhang, T.B. He, *J. Mater. Res.* 16 (2001) 1487.
- [26] R. Northhelfer-Richter, E. Klinke, C.D. Eisenbach, *Macromol. Symp.* 187 (2002) 853.
- [27] H.-Y. Nie, M.J. Walzak, N.S. McIntyre, *Polymer* 41 (2000) 2213.
- [28] A. Dasari, J. Rohrmann, R.D.K. Misra, *Mater. Sci. Eng. A* 354 (2003) 67.
- [29] A. Dasari, J. Rohrmann, R.D.K. Misra, *Mater. Sci. Eng. A* 358 (2003) 372.